Sequential ^{1}H NMR Assignments and Secondary Structure of the Kringle Domain from Urokinase

Xiang Li,[‡] Richard A. G. Smith,[§] and Christopher M. Dobson*,[‡]

Oxford Centre for Molecular Sciences and Inorganic Chemistry Laboratory, University of Oxford, South Parks Road, Oxford OX1 3QR, U.K., and SmithKline Beecham Pharmaceuticals, Great Burgh, Yew Tree Bottom Road, Epsom, Surrey KT18 5XQ, U.K.

Received March 3, 1992; Revised Manuscript Received May 18, 1992

ABSTRACT: The sequence-specific ^{1}H NMR assignments of the 89-residue recombinant kringle domain from human urokinase are presented. These were achieved primarily by utilizing TOCSY and NOESY spectra in conjunction with COSY spectra recorded at 500 MHz and 600 MHz. Regular secondary structure elements have been derived from a qualitative interpretation of nuclear Overhauser enhancement, $J_{NH\alpha}$ coupling constant, and amide proton exchange data. Two helices have been identified. One helix, involving Ser40–Gly46, corresponds to that reported for t-PA kringle 2 (Byeon et al., 1991), but does not exist in other kringles with known structures. The second helix, in the region Asn26–Gln33, is thus far unique to the urokinase kringle. Three antiparallel β-sheets and three tight turns have also been identified, which correspond exactly to those identified in t-PA kringle 2 both in solution and in the crystalline state (de Vos et al., 1992). Despite the very different ligand binding properties of the urokinase kringle, NOE data indicate that the tertiary fold of the molecule conforms closely to that found for other kringles.

Kringles are highly conserved structural motifs having a unique three-disulfide-bond triple-loop arrangement (see Figure 1) in an important family of proteins involved in hemostasis and fibrinolysis (Sottrup-Jensen et al., 1978). A single kringle domain occurs in the urinary-type plasminogen activator (urokinase, u-PA),[1] preceded by a growth factor (EGF) domain and followed by a serine protease domain. The major function of urokinase is to activate plasminogen to plasmin by limited proteolysis; the latter then catalyzes the degradation of the fibrin constituents of a blood clot. Indeed, urokinase has been found to be an effective thrombolytic agent in the treatment of acute myocardial infarction and pulmonary embolism (Haber et al., 1989). It is normally synthesized and secreted as a single-chain form (scu-PA, pro-u-PA). Although scu-PA contains some catalytic activity (Lijnen et al., 1986; Ellis et al., 1987), specific proteolytic cleavage is needed to render its full activity; the two-chain form, arising through a cleavage at Lys158, is known as high-MW urokinase (MW 54 000). Urokinase containing only the protease domain linked to a short interdomain peptide by a disulfide bridge is known as low-MW urokinase (MW 33 000), and it is catalytically fully active.

NMR studies of urokinase (Oswald et al., 1989; Bogusky et al., 1989) have revealed that distinct domains of the protein have high structural as well as motional independence. The activity of the low-MW urokinase also suggests that the protease domain possesses all the features necessary for specific recognition and cleavage of plasminogen. The EGF domain has been reported to bind the specific u-PA cellular receptors (Appella et al., 1987; Blasi, 1988), and scu-PA possesses plasminogen activation activity when bound to its receptor (Ellis et al., 1989). As the central kringle domain of urokinase does not exhibit any fibrin-binding specificity, its functional role is therefore quite different from other fibrin-binding kringles, notably certain of those in plasminogen and t-PA (Winn et al., 1980; Ramesh et al., 1986; van Zonneveld et al., 1986; Higgins & Vehar, 1987; Gething et al., 1988). Recently, it has been shown (Stephens et al., 1992) that the urokinase kringle has affinity for heparin. This suggests the possibility of a role for the interaction of the kringle with polyanions in the regulation of plasminogen activation and proteolytic activity at the extracellular matrix.

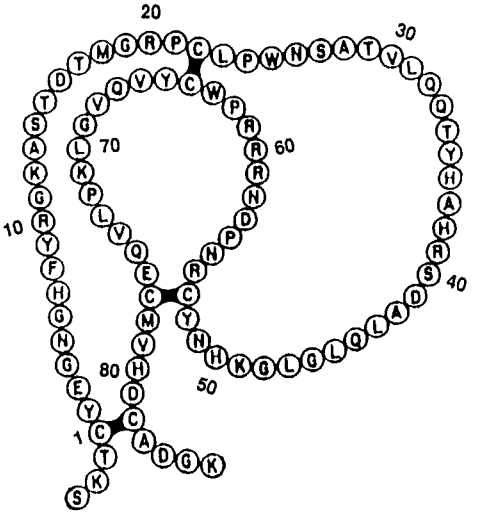

FIGURE 1: Schematic representation of the primary structure of the kringle domain of human urokinase. Disulfide bonds are indicated by thick solid lines.

* To whom correspondence should be addressed.

‡ University of Oxford.

§ SmithKline Beecham Pharmaceuticals.

[1] Abbreviations: u-kringle, urokinase kringle; t-PA, tissue-type plasminogen activator; PGK1, plasminogen kringle 1; PTK4, prothrombin kringle 4; NMR, nuclear magnetic resonance; 2D, two-dimensional; COSY, two-dimensional correlation spectroscopy; NOE, nuclear Overhauser enhancement; NOESY, two-dimensional NOE spectroscopy; TOCSY, two-dimensional total coherence spectroscopy; $d_{NN}(i,j)$, NOE connectivity between the NH proton on residue i and the NH proton on residue j; $d_{\alpha N}(i,j)$, NOE connectivity between the αCH proton on residue i and the NH proton on residue j; $d_{\alpha\alpha}(i,j)$, NOE connectivity between the αCH proton on residue i and the αCH proton on residue j; $d_{\beta N}(i,j)$, NOE connectivity between the βCH proton on residue i and the NH proton on residue j; d_{NN}, $d_{NN}(i,i+1)$; $d_{\alpha N}$, $d_{\alpha N}(i,i+1)$; $d_{\beta N}$, $d_{\beta N}(i,i+1)$; J, coupling constant.

0006-2960/92/0431-9562$03.00/0

Structural information about the kringle domain of urokinase is clearly crucial in order to define its biological role. Crystal structures of prothrombin kringle 1 (PTK1), human plasminogen kringle 4 (PGK4), and most recently t-PA kringle 2 have been solved (Park & Tulinsky, 1986; Tulinsky et al., 1988; Mulichak et al., 1991; Wu et al., 1991; de Vos et al., 1992). Solution structures of plasminogen kringle 4 and t-PA kringle 2 derived from NMR data have also been reported (Atkinson & Williams, 1990; Byeon & Llinás, 1991). Many other NMR studies have been performed on kringles 1, 4, and 5 from plasminogen (Trexler et al., 1985; De Marco et al., 1985; Llinás et al., 1983; Ramesh et al., 1986, 1987; Thewes et al., 1988, 1990; Mabbutt & Williams, 1988) and on kringle 2 of t-PA (Byeon et al., 1989, 1991). Although structurally similar, some of the kringles differ significantly in ligand-binding capacities or patterns. No crystal structure is available for either intact urokinase or its fragments. In this study, we report the ^{1}H NMR sequential assignment of the recombinant urokinase kringle domain. A total of 82 of the 89 residues of the kringle domain have been assigned using 2D homonuclear NMR methods. Of the seven remaining residues, four are residues at the N- and C-termini, outside the Cys1–Cys82 disulfide bond; the other three lie in a structurally disordered region. Secondary structure elements have been derived on the basis of the NMR data, and the tertiary fold has been characterized.

MATERIALS AND METHODS

Kringle Sample. The kringle domain used in this study was derived from recombinant scu-PA by limited proteolysis as described previously (Bogusky et al., 1989) and was kindly provided by Grünenthal GmbH, Aachen, Germany. The NMR sample was dissolved in 0.5 mL of 90% H_2O/10% D_2O, to give a final protein concentration of 4.5 mM, at pH 4.5. While HPLC analysis showed the sample to be pure, the NMR analysis indicated the existence of minor components. N-Terminal amino acid sequencing was therefore carried out and revealed that although the major portion of the molecule was intact [i.e., starting from the Ser(–3) position where the kringle was originally cleaved from the recombinant urokinase (Note that the numbering system used here assigns the first cysteine of the kringle as residue 1; plasmin cleavage of intact u-PA occurs between Lys46(–4) and Ser47(–3) in the full-length sequence)], two additional species were present. One was a fragment whose sequence begins at the Thr(–1) position; this and the intact species account for about 70% of the protein in solution. The third species was a fragment whose sequence starts at Ala13. This indicated that a proportion of the kringle sample (ca. 30%) was nicked at Lys12–Ala13, leaving 15 (or 13) N-terminal residues that are only linked to the main body of the molecule by the disulfide bridge, Cys1–Cys82. As the kringle fragment was difficult to obtain and there was only a limited quantity of sample available, further purification of the sample was not attempted after the detection of the minor species. Instead, as will be demonstrated below, the NMR spectra of the intact protein (Ser(–3)–Lys86) were analyzed in the presence of the minor species. This was possible because the effects of sample heterogeneity were found to be localized to the N-terminal region of the molecule, and the sequential assignment method could unambiguously detect the cleavage in the minor species.

NMR Spectroscopy. ^{1}H NMR spectra were recorded on a home-built GE-Nicolet 500 spectrometer equipped with an Oxford Instruments Co. magnet and a Bruker probe, and on a Bruker AM600 spectrometer, with ^{1}H resonant frequencies

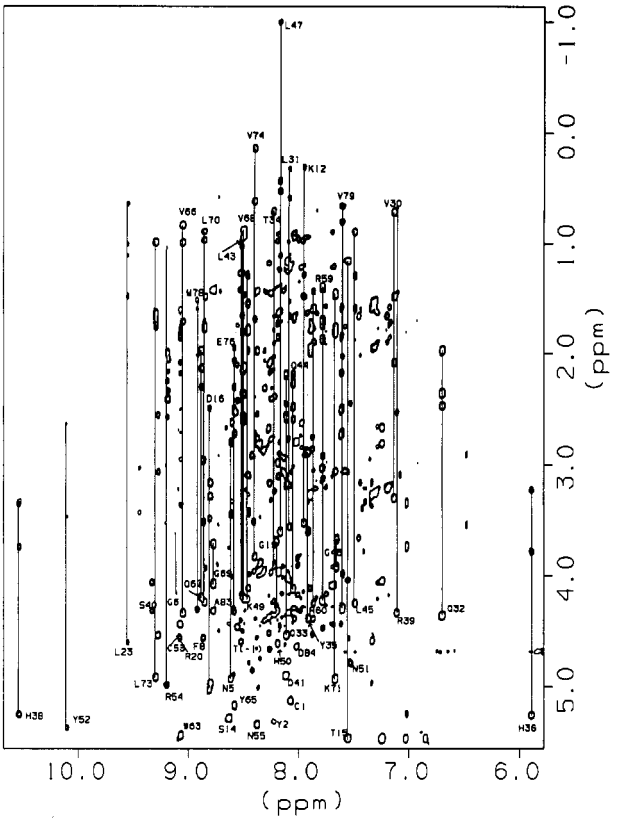

FIGURE 2: The NH/aromatic–aliphatic region of a TOCSY spectrum of u-kringle, recorded in H_2O at 35 °C, with a mixing time of 65 ms. Sequence numbers of most residues are given at the positions of either the direct NH–C_αH peaks or the most upfield cross-peaks. Examples showing the direct and relayed connectivities of the spin systems for selected residues are shown with continuous lines.

of 500.10 and 600.13 MHz, respectively. All 2D experiments were carried out at 25 °C and 35 °C using pure phase absorption mode. Quadrature detection in the $t1$ dimension was achieved by the States method (States et al., 1982) on the GE-Nicolet 500 and by the time proportional phase incrementation method (Marion & Wüthrich, 1983) on the Bruker AM600 spectrometer. For the TOCSY (Braunschweiler & Ernst, 1983; Davis & Bax, 1985) experiments, the RF pulses were generated via the attenuated low-power transmitter channel on the GE-Nicolet 500, or through reverse mode on the Bruker AM600 spectrometer (90° pulse ~25–27 μs). MLEV17 (Bax & Davis, 1985b) or WALTZ17 (Bax, 1989) spin-lock sequences bracketed by 2.0-ms trim pulses were used with mixing times of 58–64 ms. Short delays were introduced either within the composite pulses or before detection to eliminate cross-relaxation effects in the rotating frame (Griesinger et al., 1988). NOESY (Jeener et al., 1979; Macura et al., 1981) data were collected with mixing times of 120 ms and 200 ms. ROESY (Bothner-By et al., 1984; Bax & Davis, 1985a) experiments were performed with mixing times of 200 and 300 ms. For measurements in H_2O, the water resonance was suppressed by means of the 1–$\bar{1}$ "jump and return" sequence (Plateau & Gueron, 1982). In the TOCSY experiments, the spin-locked magnetization was first stored back along the Z axis using a 90° "flip-back" pulse before the 1–$\bar{1}$ pulses. Because the radiation damping acts as an additional relaxation mechanism (Abragam, 1961), which rotates the magnetization toward the $+Z$ (static field) axis, the second pulse of 1–$\bar{1}$ was set 0.15 μs shorter than the first. To minimize the radiation damping effect, the first 90° preparatory pulse in the TOCSY experiment and the mixing

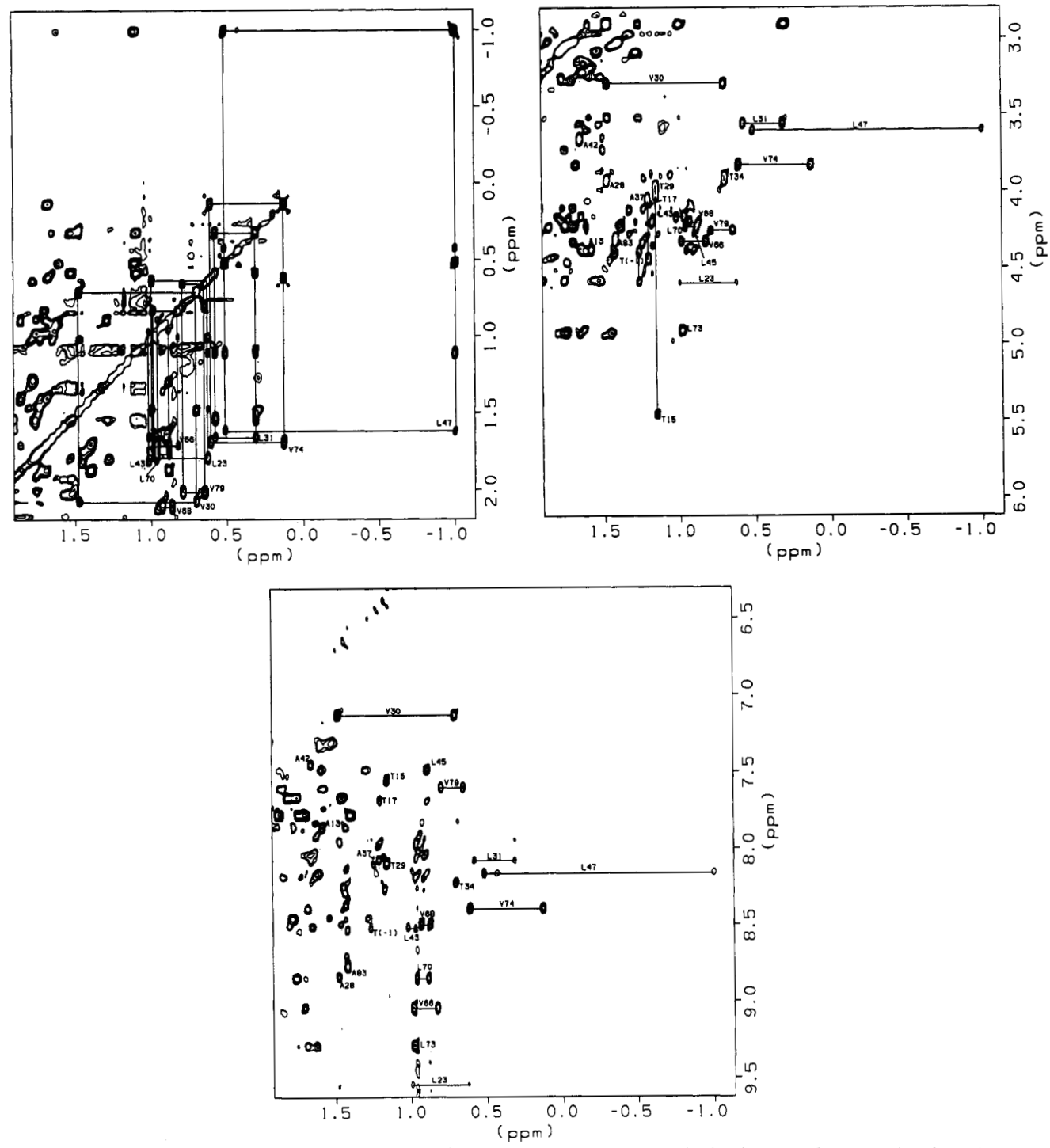

FIGURE 3: The upfield aliphatic (*F2* dimension) regions of the 65-ms TOCSY spectrum (as in Figure 2), demonstrating the assignment of Ala, Thr, Val, and Leu spin systems of u-kringle. (a, top left) Connectivities through the two $C_\beta H_3$ cross-peaks from leucine and two $C_\gamma H_3$ cross-peaks from valine to the corresponding $C_\beta H$ resonances are indicated. (b, top right) $C_\alpha H$–$C_\delta H_3$ and $C_\alpha H$–$C_\gamma H_3$ connectivities are indicated by horizontal lines for Leu and Val residues, respectively. The $C_\alpha H$–$C_\gamma H_3$ and $C_\beta H$–$C_\gamma H_3$ cross-peaks from the same Thr residue are connected by vertical lines, with sequence numbers at the positions of the $C_\alpha H$–$C_\gamma H_3$ cross-peaks. $C_\alpha H$–$C_\beta H_3$ cross-peaks from Ala are also indicated. (c, bottom) Connectivities between backbone NH and methyl proton resonances are indicated for Ala, Thr, Val, and Leu spin systems.

pulse in the NOESY experiment were phase cycled in two-step (45°) fashion, 45° out of register with the other pulses. For TOCSY experiments, additional water suppression was achieved by applying a very low level water irradiation during the relaxation delay. The receiver phase was optimized to minimize baseline distortions for both TOCSY and NOESY experiments performed on the Bruker AM600 spectrometer (Marion & Bax, 1988). Standard phase sensitive COSY (Aue et al., 1976; Bax & Freeman, 1981) and DQF-COSY (Rance et al., 1983) spectra were also collected. In these experiments, $C_\alpha H$ resonances bleached out by the strong irradiation of the H_2O peak during the relaxation delays used for solvent suppression were successfully recovered by recording a pre-TOCSY COSY spectrum (Otting & Wüthrich, 1987) under the same conditions. Typical data sets were of 350–512 complex *t*1 increments (on the Bruker spectrometer with the TPPI method, this is equivalent to NE = 700–1024) of 2K data points. The COSY spectrum used for $J_{NH\alpha}$ coupling constant measurement was of 4K data points at 25° with otherwise identical parameters. All the NMR data were

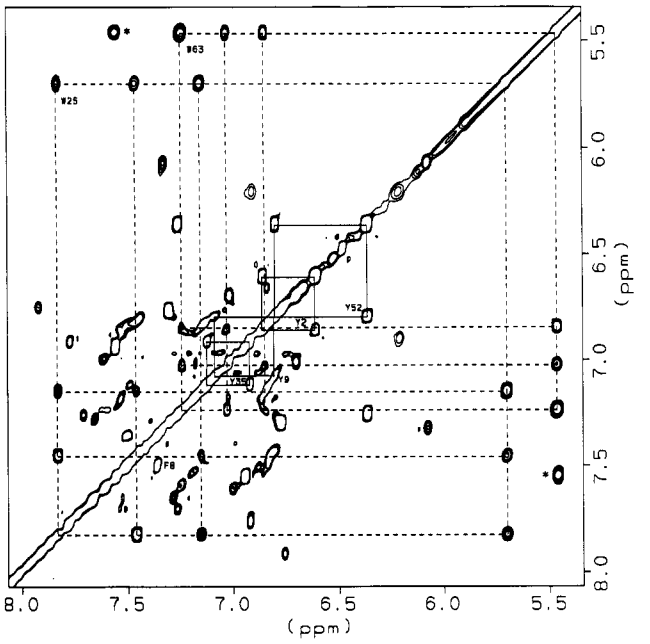

FIGURE 4: The aromatic region of the 65-ms TOCSY spectrum (as in Figure 2). The spin systems of the two Trp residues are indicated by dashed lines. The H(3,5) and H(2,6) cross-peaks from four of the Tyr residues are indicated by solid lines. The fifth Tyr residue, Tyr65, has degenerate H(3,5) and H(2,6) resonances. The only Phe residue in u-kringle, Phe8, is also indicated. Note the $C_\alpha H$ resonance of the Thr15 fingerprint peak (marked with *) has a chemical shift value (5.46 ppm) coincident to that of H5 from Trp63. Some unmarked cross-peaks in this region result from side-chain amide protons.

processed on a SUN-4 workstation using the FELIX program provided by Dr. D. R. Hare, Hare Research Inc. The dispersive residual water resonance present in the experiments with the 1–$\bar{1}$ pulse sequence was filtered out using a low-frequency notch filter in the time domain (Marion et al., 1989). All the spectra were resolution enhanced in $t2$ by trapezoidal and double-exponential weighting functions and in $t1$ by squared-sine-bell and double-exponential functions. After zero-filling, the digital resolution in both $t1$ and $t2$ dimensions was 3.5 Hz/point for data collected on the GE-Nicolet 500 and 4.2 Hz/point for data collected on the Bruker AM600.

RESULTS

Assignment of the ¹H NMR spectra of the recombinant kringle was achieved by means of standard homonuclear methods (Wüthrich, 1986; Wagner, 1990). These involve initially the identification of spin systems from different amino acid residue types via intraresidue through-bond connectivities (TOCSY, COSY); at the next stage these spin systems are allocated to specific positions in the amino acid sequence by establishing sequential interresidue through-space (<5 Å) connectivities (NOESY). This procedure, which would otherwise be conventional, was initially complicated by the 3-fold heterogeneity of the sample. However, with the result of N-terminal sequencing in mind, it was possible to assign in a sequence-specific manner virtually all the spin systems from the intact molecule by very carefully following the sequential information and examining the spectra obtained under different conditions. For the majority of the protein, with probably the exception of the first 15/13 N-terminal residues, resonances in the spectra of the three species were identical. Examples of TOCSY and NOESY spectra demonstrating some of the assignments are shown in Figures 2–6.

Identification of the Spin Systems. Our assignment of the spin systems started from the upfield aliphatic region in the

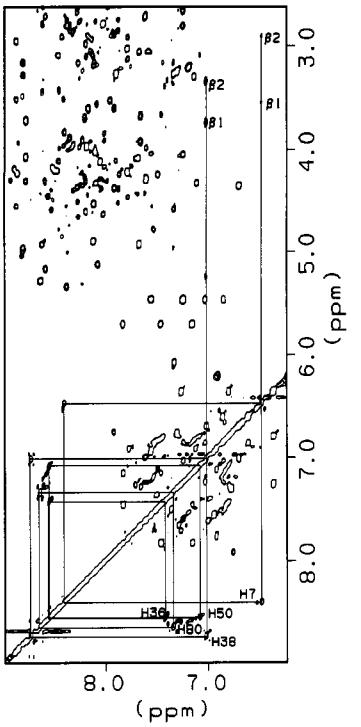

FIGURE 5: The assignment of histidine spin systems from the same TOCSY spectrum as in Figure 4. The connectivities between the two β-protons and the H4 ring protons of His7 and His38 are indicated by continuous lines.

TOCSY spectra (Figure 3a–c), where characteristic spin system patterns could be found for valine, leucine, alanine, and threonine residues. It proved possible to identify completely all 22 of these spin systems by analysis of just one TOCSY spectrum recorded in H_2O under optimal conditions. The assignment was confirmed in the low-field NH region of the same spectrum, where spin systems could be delineated starting from the backbone NH–$C_\alpha H$ cross-peaks, the so-called fingerprint peaks (Figure 2). Examination of a COSY spectrum was valuable to distinguish between direct (3-bond) peaks and more remote (relay) peaks. Some resonances from lysine spin systems were also visible in this region; full assignments of these spin systems, however, were achieved only at the later sequential stage. Identification of arginine spin systems followed the same line, albeit less successfully because of the existence of higher mobility in some of these residues (see below).

The urokinase kringle domain contains 2 tryptophans, 5 tyrosines, 5 histidines, and 1 phenylalanine. Complete spin system networks for the H4, H5, H6, and H7 ring protons from the two tryptophans were readily identified in TOCSY spectra; these are illustrated in Figure 4. Two further cross-peaks linking the imidazole NH and H2 ring protons of the two tryptophans were also observed in TOCSY and COSY spectra. Figure 4 also shows the ring proton cross-peaks from four of the tyrosines. The fifth tyrosine, Tyr65, has almost degenerate H(2,6) and H(3,5) resonances; this is supported by the observation of a sharp line with double the normal intensity for a tyrosine resonance at the corresponding position in the 1D spectrum. The cross-peaks between the H2 and H4 ring protons of histidines are normally not observed in COSY spectra, due to the small four-bond coupling of ca. 1 Hz. However, the cross-peaks between the H2 and H4 ring protons from all the five histidines can be clearly observed in the TOCSY spectrum (Figure 5) owing to its improved efficiency of coherence transfer and absorptive line shape. Furthermore, cross-peaks between $C_\beta H$ and H4 protons can even be detected

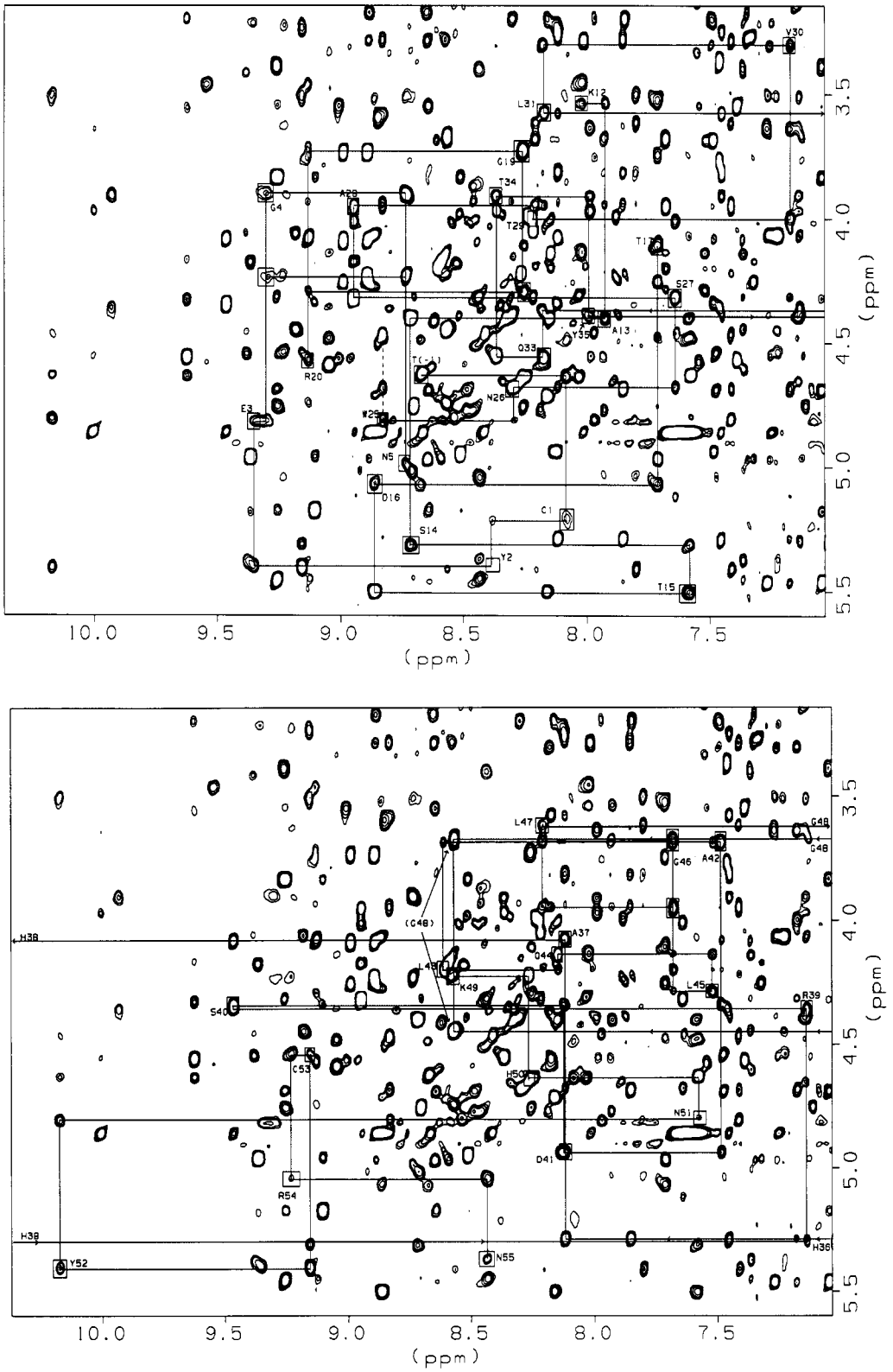

FIGURE 6: Fingerprint region of a NOESY spectrum of u-kringle, recorded in H_2O at 25 °C, with a mixing time of 200 ms. Selected stretches of sequential $d_{\alpha N}(i,i+1)$ connectivities are indicated by solid lines. Dashed lines are used to indicate $d_{\alpha N}(i,i+1)$ connectivities between Pro(i) and its following residue. NH–C_αH cross-peaks from Q32, H36, and H38 lie outside the regions illustrated in the plots. The direct intraresidue NH(i)–C_αH(i) cross-peaks are boxed and labeled with residue type and sequence number. (a, top) T(−1)–N5, K12–T17, G19–R20, P24–L31, and Q33–Y35. (b, bottom) H36–N55.

for His7 and His38 (Figure 5); similar observations have previously been made in the spectra of small peptides (Bax, 1989). Identification of the links between ring protons and the backbone C_βH protons for histidine is important, in contrast to the situation for other aromatic residues, as such information is difficult to obtain from NOESY spectra for histidine residues. The assignment of the only phenylalanine residue in the urokinase kringle is also shown in Figure 4. Here, again, H4 and H(2,6) protons have almost degenerate resonances.

It was relatively straightforward to assign many of the AMX and AMPTX spin systems starting from the low-field NH

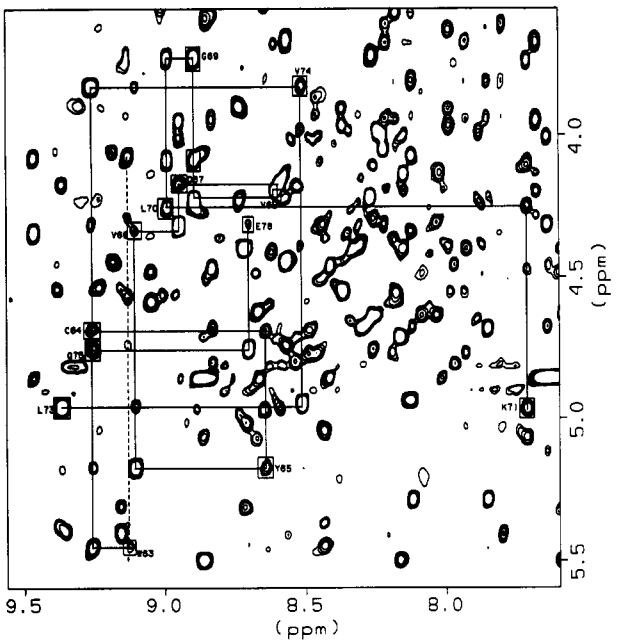

FIGURE 7: Part of the fingerprint region of the NOESY spectrum (as in Figure 6) of u-kringle in H_2O. The sequential connectivities for the third β-sheet region (P62–K71 and L73–E76) are indicated.

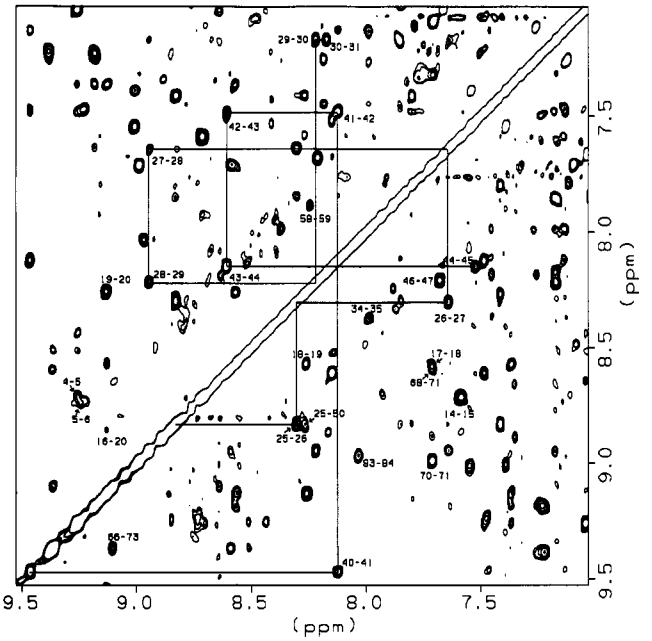

FIGURE 8: The NH–NH region of the NOESY spectrum (as in Figure 6) of u-kringle in H_2O. Sequential NH(i)–NH(i+1) NOEs are indicated for selected residues. Consecutive $d_{NN}(i,i+1)$ connectivities found in the two helical regions (W25-Q33 and S40-G46) are indicated by solid lines.

region of the TOCSY spectra. However, unlike the situation for the spin systems described above, more than the expected number of such spin systems could be observed in the TOCSY spectra because of the heterogeneity of the sample. Unambiguous identification of most of these spin systems was not achieved at this stage, but the corresponding amino acid type and sequence position became clear during the sequential assignment stage.

No attempt was made to assign proline residues at this stage. They were identified only after the completion of the sequence-specific assignment in the corresponding regions, with the aid of sequential information provided by NOESY spectra.

Sequential Assignment. The sequence-specific assignment of the kringle spectra was accomplished primarily by establishing standard $d_{\alpha N}(i,i+1)$ and $d_{NN}(i,i+1)$ sequential connectivities. The successful assignment of many spin systems from aliphatic (i.e., Ala, Thr, Val, Leu) and aromatic residues provided many starting points for this analysis. Examples of NOESY spectra showing the sequential assignment of many residues are given in Figures 6–8. The assignment of the N-terminal region proved to be significantly more difficult than that of the center regions of the sequence, partly because of the cleavage at Lys12–Ala13 in part of the sample, which resulted in reduced intensities of the intraresidue cross-peaks from this region. Another likely reason for the weak NOE signals is that there is substantial local mobility of residues or conformational disorder in the terminal regions. If these parts of the molecule reorientate at a rate, $\tau'_c{}^{-1}$, close to the resonant frequency, ω_0, the NOE signals will become very small (theoretically, when $\omega_0\tau'_c = \sqrt{5}/2$, NOEs vanish). Nevertheless it is still possible, by carefully examining all the sequential NOE information available in NOESY spectra recorded at different temperatures (25 °C and 35 °C) and frequencies (500 MHz and 600 MHz), to trace the connectivities from Thr(−1), the only threonine residue left after successful sequential assignment of the other regions, to Phe8, the only phenylalanine residue. The sequential assignment was extended from Phe8 to Gly11 which had been sequentially assigned from the opposite direction; this confirmed again the assignment of this region. The Glu3 fingerprint peak could not, in fact, be observed in the spectra recorded at 35 °C (the temperature used for the main assignment work) as it lies exactly on the water resonance. It was not detected in the pre-TOCSY COSY spectrum either, because of its weak intensity. A weak cross-peak just above the water resonance, however, could be observed in a NOESY spectrum at 25 °C, with a sequential $d_{\alpha N}(i,i+1)$ peak to Gly4, and a $d_{\alpha N}(i-1,i)$ peak to Tyr2. Inspection of a TOCSY spectrum recorded at the same temperature revealed a weak AMPTX spin system at exactly the same position. This is an example of the assignment of a spin system which remained undetected until a very late stage.

The assignment of the C-terminal region suffered from problems similar to those of the N-terminal region in that intraresidue cross-peaks, especially in the NOESY spectra, were weak or missing. This is likely to be a consequence of the fact that this region is linked to the N-terminal region by a disulfide bond (C1–C82). The strategy described above for the N-terminal region was again adopted and permitted assignment to be achieved. In the case where sequential information is also lost, spin systems could be assigned through elimination; this applied to the assignment of His80, the only remaining histidine after successful sequential assignment in the other regions.

The third region of the molecule that proved difficult to assign is a seven-residue stretch between Pro56 and Pro62. Here, the three consecutive arginines at positions 59–61 make it a highly positively charged cluster. Although very strong cross-peaks are observed for the arginines in all the TOCSY spectra, their NOE signals are barely observed in the NOESY spectra. The absence of NOE signals cannot be attributed to sample heterogeneity. Instead, it is likely to originate solely from the dynamical behavior of this region which appears similar to that described for the N-terminal region. This indicates that this part of the molecule may have much higher mobility than the main body of the molecule. One would expect this phenomenon to be temperature-dependent and field-strength-dependent; whereas this is indeed the case, the

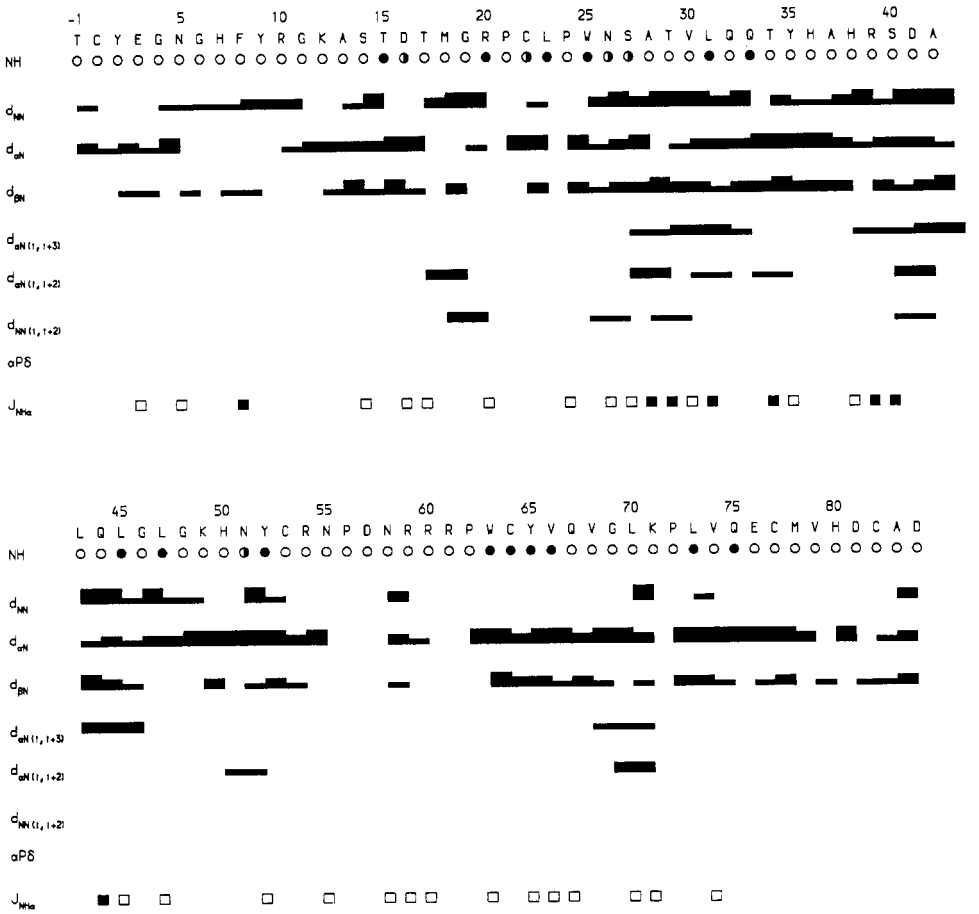

FIGURE 9: Sequence of u-kringle, together with a summary of all the short- and medium-range NOEs involving the NH, $C_\alpha H$, and $C_\beta H$ as well as the $C_\delta H$ protons of proline residues. Filled, half-filled, and empty circles indicate amides with slow (≥20 h), medium (≥6 h), and fast (<10 min) exchange rates, respectively, at pH 4.5, 25 °C. The NOEs are classified as strong, medium, and weak by the thickness of the lines. Filled and open boxes indicate, respectively, $J_{NH\alpha}$ coupling constants of less than 7 Hz or larger than 8 Hz.

ranges of temperature (25 °C/35 °C) and field strength (500 MHz/600 MHz) explored are not wide enough to resolve the problems raised. ROESY experiments (with mixing times of 200 and 300 ms) were used to address the problem, but they failed to yield any new information. Conformational disorder is therefore likely to be the reason for the absence of NOEs/ROEs in this region. Thus, to date, there are still three residues remaining unassigned in this region. Except for these three residues and part of Pro21 (whose resonances are close to the water resonance), all residues between T(−1) and D(84) have been assigned. The sequential and medium-range NOEs involving NH, $C_\alpha H$, and $C_\beta H$ as well as the $C_\delta H$ of proline are summarized in Figure 9. A list of assignments is given in Table I.

Identification of Secondary Structure. Regular secondary structure elements are usually derived from a qualitative interpretation of the NOEs, $J_{NH\alpha}$ coupling constants, and hydrogen exchange rates (Wüthrich, 1986; Wagner, 1990). $J_{NH\alpha}$ coupling constants of 34 residues were calculated by fitting the cross-sections of the NH–$C_\alpha H$ cross-peaks from a 4K COSY spectrum recorded at 25 °C (Redfield & Dobson, 1990; Smith et al., 1991). Hydrogen exchange rates were monitored initially by recording a set of 12 1D spectra in the first half hour after dissolving the sample, freshly lyophilized from H_2O, into D_2O and then by recording a COSY and a NOESY spectrum. The results, together with data for $J_{NH\alpha}$ coupling constants, are also presented in Figure 9.

Two helical regions involving Asn26–Gln33 and Ser40–Gly46 can be identified on the basis of consecutive strong-$d_{NN}(i,i+1)$ (except $d_{NN}(45,46)$, which is weak) and medium-range $d_{\alpha N}(i,i+3)$ connectivities (Figure 8). The identification is further supported by the prevalence of generally smaller (<7 Hz) $J_{NH\alpha}$ coupling constants which are usually associated with a helical conformation. The repeated occurrence of $d_{\alpha N}(i,i+2)$ as well as $d_{NN}(i,i+2)$ connectivities along the first helix (Asn26–Gln33) suggests that this is probably closer to a 3_{10}-helix than to an α-helix.

Three antiparallel β-sheet structures have been deduced on the basis of strong consecutive sequential $d_{\alpha N}(i,i+1)$ connectivities (Figure 9) and long-range interstrand $d_{NN}(i,j)$, $d_{\alpha N}(i,j)$, and $d_{\alpha\alpha}(i,j)$ NOEs. The first β-sheet comprises two short strands: Thr15–Asp16 and Arg20–Pro21–Cys22 (Figure 10A). The second β-sheet is also formed by two short stretches of polypeptide chain: Pro24–Trp25 and His50–Asn51 (Figure 10B). The third β-sheet involves residues Trp63–Gln67 and Pro72–Gln76 (Figure 10C). Large (>8 Hz) $J_{NH\alpha}$ coupling constants and retarded amide proton exchange rates found in these regions of the protein are consistent with these findings.

A β-hairpin tight turn is anticipated involving the pentapeptide, Asp16–Thr17–Met18–Gly19–Arg20, as it connects the two neighboring strands of the first β-sheet identified above. This expectation is confirmed by the observation of a medium $d_{\alpha N}(17,19)$ cross-peak together with strong consecutive $d_{NN}(i,i+1)$ cross-peaks (i runs from 17 to 19). Similarly, a reverse turn is located in the tetrapeptide, Val68–Gly69–Leu70–Lys71, which links the two neighboring strands of the third β-sheet. The strong $d_{\alpha N}(69,70)$ and $d_{NN}(70,71)$ cross-peaks, together with a medium $d_{\alpha N}(69,71)$ cross-peak, imply this is either a type II turn or a half-turn. It is worth noting that whereas the observed weak $d_{NN}(69,70)$ cross-peak may support

Table I: ^{1}H Chemical Shifts of Urokinase Kringle at 35 °C, pH 4.5

residue	NH	αH	βH	others	residue	NH	αH	βH	others
Thr(−1)	8.53	4.59	4.40	$^{\gamma}CH_3$ 1.26	Leu43	8.52	4.17	1.81, 1.66	$^{\gamma}CH$ 1.76; $^{\delta}CH_3$ 1.03, 0.96
Cys1	8.08	5.12	3.19, 3.07		Gln44	8.05	4.12	2.26, 2.18	$^{\gamma}CH_2$ 2.59, 2.47
Tyr2	8.23	5.31	3.17, 2.59	H(2,6) 6.61; H(3,5) 6.86	Leu45	7.49	4.24	1.59	$^{\gamma}CH$ 1.29; $^{\delta}CH_3$ 0.89, 0.89
Glu3	9.18	4.81	2.32, 2.05	$^{\gamma}CH_2$ 2.40, 2.16	Gly46	7.66	3.92, 3.68		
Gly4	9.15	4.21, 3.90			Leu47	8.17	3.61	1.61, 0.42	$^{\gamma}CH$ 1.11; $^{\delta}CH_3$ 0.52, −1.00
Asn5	8.62	4.93	3.44, 2.79	$^{\gamma}NH_2$ 7.22, 7.11	Gly48	5.41	4.38, 3.67		
Gly6	9.15	4.20, 3.62			Lys49	8.47	4.20	1.77	$^{\gamma}CH_2$ 1.55, 1.29; $^{\delta}CH_2$ 1.80; $^{\epsilon}CH_2$ 3.09
His7	8.73	4.49	3.53, 2.92	H2 8.40; H4 6.48	His50	8.19	4.61	3.11, 2.98	H2 8.54; H4 7.08
Phe8	8.87	4.56	3.52, 2.96	H(2,6) 7.51; H(3,5) 7.36; H4 7.49	Asn51	7.53	4.79	3.06, 2.44	$^{\gamma}NH_2$ 7.40
Tyr9	7.54	4.56	2.99, 2.92	H(2,6) 6.81; H(3,5) 7.09	Tyr52	10.10	5.37	3.46, 2.62	H(2,6) 6.36; H(3,5) 6.79
Arg10	8.46	4.11	1.99, 1.94	$^{\gamma}CH_2$ 1.78, 1.71; $^{\delta}CH_2$ 3.27; NH 7.90, 7.34	Cys53	9.11	4.45	3.22, 2.69	
Gly11	4.47	4.12, 3.44			Arg54	9.19	4.49	1.97, 1.05	$^{\gamma}CH_2$ 2.57, 1.49; $^{\delta}CH_2$ 3.02; NH 7.48
Lys12	7.95	3.53	1.27	$^{\gamma}CH_2$ 1.00, 0.31; $^{\delta}CH_2$ 1.48; $^{\epsilon}CH_2$ 2.90	Asn55	8.38	5.34	2.54, 1.97	$^{\gamma}NH_2$ 7.37
Ala13	7.87	4.38	1.58		Pro56				
Ser14	8.63	5.28	4.43, 3.75		Asp57				
Thr15	7.55	5.46	4.04	$^{\gamma}CH_3$ 1.15	Asn58	8.18	3.96	2.90, 2.79	
Asp16	8.81	5.03	3.49, 2.49		Arg59	7.78	4.22	1.88, 1.74	$^{\gamma}CH_2$ 1.69, 1.40; $^{\delta}CH_2$ 3.03
Thr17	7.68	4.08	4.44	$^{\gamma}CH_3$ 1.21	Arg60	7.87	4.24	1.90, 1.77	$^{\gamma}CH_2$ 1.61, 1.44; $^{\delta}CH_2$ 3.05
Met18	8.51	4.41	2.35, 2.15	$^{\gamma}CH_2$ 2.60, 2.55	Arg61				
Gly19	8.20	4.29, 3.70			Pro62		4.11	2.29	$^{\gamma}CH_2$ 2.26, 2.16; $^{\delta}CH_2$ 3.92, 3.74
Arg20	9.08	4.57	2.17, 2.07	$^{\gamma}CH_2$ 1.78, 1.64; $^{\delta}CH_2$ 3.43, 3.03	Trp63	9.07	5.43	3.36, 2.95	H4 7.03; H5 5.46; H6 7.24; H7 6.85
Pro21		4.71							H2 7.34; NH(*i*) 10.79
Cys22	8.11	4.53	3.17, 2.58		Cys64	9.23	4.69	3.52, 3.01	
Leu23	9.55	4.59	1.48, 1.79	$^{\gamma}CH$ 1.11; $^{\delta}CH_3$ 1.00, 0.63	Tyr65	8.59	5.17	2.92, 2.52	H(2,6) 6.96; H(3,5) 6.98
Pro24		4.44	1.88	$^{\gamma}CH_2$ 2.20, 2.05; $^{\delta}CH_2$ 3.79, 3.51	Val66	9.05	4.33	1.71	$^{\gamma}CH_3$ 0.99, 0.83
Trp25	8.77	4.80	3.92, 3.28	H4 7.83; H5 7.15; H6 5.70; H7 7.45	Gln67	8.89	4.19	2.12	$^{\gamma}CH_2$ 2.29, 1.97; $^{\gamma}NH_2$ 7.26, 6.36
				H2 7.38; NH(*i*) 11.70	Val68	8.50	4.21	2.12	$^{\gamma}CH_3$ 0.94, 0.88
Asn26	8.27	4.66	3.17, 2.16	$^{\gamma}NH_2$ 7.77, 6.91	Gly69	8.78	4.07, 3.72		
Ser27	7.61	4.30	3.98, 3.98		Leu70	8.86	4.23	1.76	$^{\gamma}CH$ 1.70; $^{\delta}CH_3$ 0.97, 0.89
Ala28	8.85	3.93	1.48		Lys71	7.67	4.92	1.81	$^{\gamma}CH_2$ 1.77, 1.45; $^{\delta}CH_2$ 1.47; $^{\epsilon}CH_2$ 3.06
Thr29	8.10	4.02	3.97	$^{\gamma}CH_3$ 1.15	Pro72		4.94	1.52	$^{\gamma}CH_2$ 1.99, 1.78; $^{\delta}CH_2$ 3.73, 3.65
Val30	7.14	3.30	2.08	$^{\gamma}CH_3$ 1.48, 0.71	Leu73	9.30	4.91	1.69, 1.63	$^{\gamma}CH$ 1.76; $^{\delta}CH_3$ 0.98, 0.98
Leu31	8.09	3.56	1.65, 1.09	$^{\gamma}CH$ 1.52; $^{\delta}CH_3$ 0.58, 0.32	Val74	8.40	3.83	1.69	$^{\gamma}CH_3$ 0.62, 0.14
Gln32	6.70	4.36	1.97	$^{\gamma}CH_2$ 2.46, 2.35; $^{\gamma}NH_2$ 7.18, 7.03	Gln75	9.19	4.77	1.98, 1.04	$^{\gamma}CH_2$ 2.56, 2.24; $^{\gamma}NH_2$ 7.02, 6.70
Gln33	8.11	4.53	2.57, 2.18	$^{\gamma}CH_2$ 2.44	Glu76	8.59	4.31	2.06, 1.95	$^{\gamma}CH_2$ 2.49, 2.29
Thr34	8.23	3.91	3.94	$^{\gamma}CH_3$ 0.70	Cys77	8.42	4.85	2.91, 2.91	
Tyr35	7.91	4.38	3.60, 2.89	H(2,6) 7.12; H(3,5) 6.91	Met78	8.56	4.46	2.10	$^{\gamma}CH_2$ 2.03, 2.41
His36	5.90	5.26	3.78, 3.23	H2 8.54; H4 7.42	Val79	7.61	4.27	2.02	$^{\gamma}CH_3$ 0.80, 0.66
Ala37	8.08	4.05	1.21		His80	8.73	4.49	3.55, 2.92	H2 8.63, H4 7.34
His38	10.54	5.24	3.74, 3.34	H2 8.72; H4 7.02	Asp81	8.61	4.75	3.33, 2.61	
Arg39	7.11	4.33	2.51, 1.45	$^{\gamma}CH_2$ 0.67; $^{\delta}CH_2$ 3.89, 2.87; NH 9.90, 6.94	Cys82	8.26	4.53	3.32, 2.78	
Ser40	9.33	4.31	4.05, 4.05		Ala83	8.78	4.31	1.42	
Asp41	8.12	4.90	3.19, 2.56		Asp84	8.02	4.03	2.79, 2.79	
Ala42	7.46	3.66	1.66						

a type II turn, the $J_{NH\alpha}$ coupling constant of 7.9 Hz found for the third residue Leu70 would suggest some conformational averaging between the two types of turns. The same phenomenon is also observed in t-PA kringle 2. A third reverse turn is identified involving residues Pro24–Trp25–Asn26–Ser27. Weak $d_{NN}(25,27)$, medium $d_{NN}(25,26)$, and strong $d_{NN}(26,27)$ connectivities found in this segment suggest the formation of either a type I or type I′ turn. Although the proximity of the NH–C$_\alpha$H cross-peak of Trp25 to the water resonance precludes a reliable measurement of $J_{NH\alpha}$ for this residue, the value of $J_{NH\alpha}$ (ca. 10 Hz) found for Asn26 supports the assignment of a type I turn.

DISCUSSION

We have presented in this paper assignments for almost all the residues in the urokinase kringle sequence. On the basis of a qualitative analysis of NOE data, together with the results of $J_{NH\alpha}$ coupling constants and hydrogen exchange rates, the secondary structure elements have also been determined. Overall, the urokinase kringle domain consists of 18% helical structure and 21% β-sheet structure, a percentage slightly higher than found for other kringles. The secondary structure of the molecule is remarkably similar to that of t-PA kringle 2. β-Sheets and reverse turns identical to those found in t-PA kringle 2 were also identified in the urokinase kringle. The NOE pattern and even the chemical shifts for the many residues which are conserved in the two kringles are also similar. This similarity is also reflected in the primary sequence of the two kringles, with a figure of 46% sequence identity. The β-sheets and turns identified in the urokinase kringle also correspond reasonably well to those found in PTK1

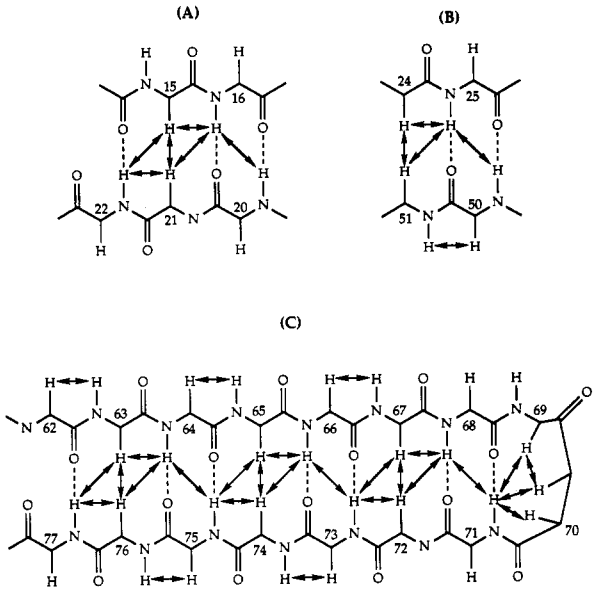

FIGURE 10: Schematic representation of the β-sheet structures identified in u-kringle. NOEs which constrain the β-sheets are denoted by arrows (↔); H-bonds are denoted by dashed lines.

(32% sequence identity) and PGK4 (34% sequence identity). An α-helical structure found in the S43–A44–Q44a–A44b–L44c–G45 segment of the t-PA kringle 2 corresponds to the α-helical structure involving S40–D41–A42–L43–Q44–L45–G46 in the urokinase kringle. As no helical structure has been reported for PTK1 and PGK4, this appears to be a unique feature for the family of kringles from plasminogen activators. The backbone amide proton exchange rates in this region are sufficiently high to suggest that this helix is at least partially exposed to solvent. A noticeable difference between the urokinase kringle and t-PA kringle 2 is the presence of another helical structure comprising residues S27–A28–T29–V30–L31–Q32–Q33 in the former. By contrast, three consecutive turns, with each one overlapping the other, were reported for the corresponding region in the t-PA kringle 2. The NOE data for the urokinase kringle suggest that this may be a 3_{10}-helix rather than an α-helix. Unlike the other helix in the urokinase kringle, our hydrogen exchange data suggest that this helix is somewhat buried in the interior of the molecule; indeed preliminary studies of long-range NOEs suggest that it participates in the formation of the hydrophobic core (see below).

A $d_{\alpha N}(53,64)$ cross-peak has been observed, connecting Cys53 and Cys64 and thus providing evidence for the close proximity of the two inner loop disulfides, Cys22–Cys64 and Cys53–Cys77. The formation of the four-sulfur cluster is reported for other kringles (Park & Tulinsky, 1986; Tulinsky et al., 1988; Mulichak et al., 1991) and is believed to serve as the core of the kringle fold. A number of NOEs involving both backbones and side chains of T17 and Q75, E76 and Cys77 require that the first and third β-sheets are in close contact, another common feature among kringles. Many long-range NOEs, notably involving Trp25, Leu31, Tyr35, His38, Leu47, Tyr52, and Trp62, provide evidence that a hydrophobic core similar to those described for other kringles exists in the urokinase kringle. This core appears to be formed primarily as a result of interactions between aromatic rings and bulky lipophilic sidechains. Experiments performed at near-neutral pH for intact urokinase showed that most features of the NMR spectra collected at pH 4.5 were retained, suggesting that the structure of the protein remains largely unperturbed when raising the pH value (Oswald et al., 1989). This is probably also true for its kringle domain, for which spectra collected at ca. pH 6 were closely similar to those collected at pH 4.5.

We have seen that three regions of the molecule exhibit local dynamical disorder. One of these, the Pro56–Pro62 cluster, contains three consecutive arginine residues, and thus is highly positively charged. This part must be exposed to solvent, and it is likely to have major functional importance (see below). The other two are the N- and C-terminal regions. The dynamical properties of the N-terminal region may imply it is part of the interface between the kringle domain and the growth factor (EGF) domain; in a combined EGF–kringle fragment this region may well be stabilized. Because of the flexibility of the terminal regions, they appear to be of little structural importance. In this regard, it is interesting to see that the partial cleavage at Lys12–Ala13 in our sample had only very local conformational effects. Indeed, the formation of a β-sheet structure starting at Thr15, and its interaction with the third β-sheet at the C-terminus of the kringle, constitute the major stabilizing forces in this region and effectively prevent the propagation of the adverse effects of the N-terminal cleavage. The small fragment (Ser(–3)/Thr(–1)–Lys(12)) cleaved at the N-terminus is virtually free, linked only to the main body of the molecule by a disulfide bond (Cys1–Cys82). Consistent with this is the observation that, in the TOCSY and COSY spectra, a number of spin systems were clustered at near random coil chemical shift positions and had strong temperature dependences of amide chemical shifts. Furthermore, such spin systems were normally not detected in NOESY spectra, suggesting that they have very different dynamical properties from those of other residues.

Despite the high sequence and structural homology between the urokinase kringle and t-PA kringle 2, their binding properties differ markedly. t-PA kringle 2 is known to have high affinity to fibrin, L-lysine, and analogous ligands, whereas the urokinase kringle has recently been reported to bind heparin-like polyanionic macromolecules (Stephens et al., 1992). The negatively charged Asp57 residue in t-PA kringle 2 which is important for lysine binding is not present in the urokinase kringle. Instead, three consecutive arginines at corresponding (59–61) locations in the urokinase kringle completely change the electrostatic properties in this region and render it impossible for the urokinase kringle to bind a zwitterionic ligand like L-lysine. This feature is, however, a plausible site for binding of an anionic ligand such as heparin. Our NMR data suggest that this region of the molecule is exposed to the solvent and in a conformationally disordered state. It can be anticipated that binding to a specific ligand would stabilize this part of the molecule, as has been found in NMR studies of other kringles in the presence of ligands. Interestingly, although His31–Lys35 has been shown to form part of the binding site in PGK4, and the binding of t-PA kringle 2 involves Lys34 [the numbering follows that of Byeon et al. (1991)], in the urokinase kringle the corresponding region is in a helical conformation and relatively buried in the interior of the molecule. Another segment which might participate in the binding of the urokinase kringle to heparin is His36–Arg39. The unambiguous characterization of the binding site, however, must await detailed 3D structure calculations.

ACKNOWLEDGMENT

We greatly enjoyed many stimulating discussions and practical assistance from Dr. A. Teuten and U. Nowak. Drs. J. Boyd, P. Driscoll, and N. Soffe helped with the NMR experiments. We are indebted to Dr. C. Redfield for valuable

suggestions and help with the program for extracting $^3J_{NH\alpha}$ coupling constants, to A. Willis for performing the N-terminal sequencing, to Dr. M. Bogusky for assistance in the initial stages of the project, and to Professor M. Llinás for providing information on the heparin/kringle interaction prior to publication. We thank Grünenthal GmbH, Aachen, Germany, for providing us with the recombinant urokinase kringle sample. C.M.D. is a member of the Oxford Centre for Molecular Sciences.

REFERENCES

Abragam, A. (1961) *Principles* of *Nuclear Magnetism*, Oxford Univ. Press, Oxford.
Appella, E., Robinson, E. A., Ullrich, S. J., Stopelli, M. P., Corti, A., Cassani, G., & Blasi, F. (1987) *J. Biol. Chem. 262*, 4437–4440.
Atkinson, R. A., & Williams, R. J. P. (1990) *J. Mol. Biol. 212*, 541–552.
Aue, W. P., Bartholdi, E., & Ernst, R. R. (1976) *J. Chem. Phys. 64*, 2229–2246.
Bax, A. (1989) *Methods Enzymol. 176*, 151–168.
Bax, A., & Freeman, R. (1981) *J. Magn. Reson. 44*, 542–561.
Bax, A., & Davis, D. G. (1985a) *J. Magn. Reson. 63*, 207–213.
Bax, A., & Davis, D. G. (1985b) *J. Magn. Reson. 65*, 335–360.
Blasi, F. (1988) *Fibrinolysis 2*, 73–84.
Bogusky, M. J., Dobson, C. M., & Smith, R. A. G. (1989) *Biochemistry 28*, 6728–6735.
Bothner-By, A. A., Stephens, R. L., Lee, J., Warren, C. D., & Jeanloz, R. W. (1984) *J. Am. Chem. Soc. 106*, 811–813.
Braunschweiler, L., & Ernst, R. R. (1983) *J. Magn. Reson. 53*, 521–528.
Byeon, I. L., & Llinás, M. (1991) *J. Mol. Biol. 222*, 1035–1051.
Byeon, I. L., Kelley, R. F., & Llinás, M. (1989) *Biochemistry 28*, 9350–9360.
Byeon, I. L., Kelley, R. F., & Llinás, M. (1991) *Eur. J. Biochem. 197*, 155–165.
Davis, D. G., & Bax, A. (1985) *J. Am. Chem. Soc. 107*, 2821–2822.
De Marco, A., Pluck, N. D., Banyai, L., Trexler, M., Laursen, R. A., Patthy, L., Llinás, M., & Williams, R. J. P. (1985) *Biochemistry 24*, 748–753.
De Vos, A. M., Ultsch, M. H., Kelley, R. F., Padmanabhan, K., Tulinsky, A., Westbrook, M. L., & Kossiakoff, A. A. (1992) *Biochemistry 31*, 270–279.
Ellis, V., Scully, M. F., Kakkar, V. V. (1987) *J. Biol. Chem. 262*, 14998–15003.
Ellis, V., Scully, M. F., Kakkar, V. V. (1989) *J. Biol. Chem. 264*, 2185–2188.
Gething, M.-J., Adler, B., Boose, J.-A., Gerard, R. D., Madison, E. L., McCookey, D., Meidell, R. S., Roman, L. M., & Sambrook, J. (1988) *EMBO J. 7*, 2731–2740.
Griesinger, C., Otting, G., Wüthrich, K., & Ernst, R. R. (1988) *J. Am. Chem. Soc. 110*, 7870–7872.
Haber, E., Quertermous, T., Matsueda, G. R., & Runge, M. S. (1989) *Science 243*, 51–56.
Higgins, D. L., & Vehar, G. A. (1987) *Biochemistry 26*, 7786–7791.
Jeener, J., Meier, B. H., Bachmann, P., & Ernst, R. R. (1979) *J. Chem. Phys. 71*, 4546–4553.
Lijnen, H. R., Zamarron, C., Blaber, M., Winkler, M. E., & Collen, D. (1986) *J. Biol. Chem. 261*, 1253–1258.
Llinás, M., De Marco, A., Hochschwender, S. M., & Laursen, R. A. (1983) *Eur. J. Biochem. 135*, 379–391.
Mabbutt, B. C., & Williams, R. J. P. (1988) *Eur. J. Biochem. 170*, 539–548.
Macura, C., Huang, Y., Suter, D., & Ernst, R. R. (1981) *J. Magn. Reson. 43*, 259–281.
Marion, D., & Wüthrich, K. (1983) *Biochem. Biophys. Res. Commun. 113*, 967–974.
Marion, D., & Bax, A. (1988) *J. Magn. Reson. 79*, 352–356.
Marion, D., Ikura, M., & Bax, A. (1989) *J. Magn. Reson. 84*, 425–430.
Mulichak, A. M., Tulinsky, A., & Ravichandran, K. G. (1991) *Biochemistry 30*, 10576–10588.
Oswald, R. E., Bogusky, M. J., Bamberger, M., Smith, R. A. G., & Dobson, C. M. (1989) *Nature 337*, 579–582.
Otting, G., & Wüthrich, K. (1987) *J. Magn. Reson. 75*, 546–549.
Park, C. H., & Tulinsky, A. (1986) *Biochemistry 25*, 2977–2982.
Plateau, P., & Gueron, M. (1982) *J. Am. Chem. Soc. 104*, 7310–7311.
Ramesh, V., Gyenes, M., Patthy, L., & Llinás, M. (1986) *Eur. J. Biochem. 159*, 581–595.
Ramesh, V., Petros, A. M., Llinás, M., Tulinsky, A., & Park, C. H. (1987) *J. Mol. Biol. 198*, 481–498.
Rance, M., Sørensen, O. W., Bodenhausen, G., Wagner, G., Ernst, R. R., & Wüthrich, K. (1983) *Biochem. Biophys. Res. Commun. 117*, 479–485.
Redfield, C., & Dobson, C. M. (1990) *Biochemistry 29*, 7201–7214.
Saudek, V., Vormald, M. R., Williams, R. J. P., Boyd, J., Stefani, M., & Ramponi, G. (1989) *J. Mol. Biol. 207*, 405–415.
Sibanda, B. L., & Thornton, J. M. (1985) *Nature 316*, 170–174.
Smith, L. J., Sutcliffe, M. J., Redfield, C., & Dobson, C. M. (1991) *Biochemistry 30*, 987–996.
Sottrup-Jensen, L., Claeys, H., Zajdel, M., Petersen, T. E., & Magnusson, S. (1978) in *Progress in Chemical Fibrinolysis and Thrombolysis* (Davidson, J. F., et al., Eds.) Vol. 3, pp 191–209, Raven, New York.
States, D. J., Haberkorn, R. A., & Ruben, D. J. (1982) *J. Magn. Reson. 48*, 286–292.
Stephens, R. W., Bokman, A. M., Myöhänen, H. T., Reisberg, T., Tapiovaara, H., Pedersen, N., Grøndahl-Hansen, J., Llinás, M., & Vaheri, A. (1992) *Biochemistry 31*, 7572–7579.
Thewes, T., Ramesh, V., Simpaceanu, E., & Llinás, M. (1988) *Eur. J. Biochem. 175*, 237–249.
Thewes, T., Constantine, K., Byeon, I. L., & Llinás, M. (1990) *J. Biol. Chem. 265*, 3906–3915.
Trexler, M., Banyai, L., Patthy, L., Pluck, N. D., & Williams, R. J. P. (1985) *Eur. J. Biochem. 152*, 439–446.
Tulinsky, A., Park, C. H., & Skrzypczak-Jankun, E. (1988) *J. Mol. Biol. 202*, 885–901.
Van Zonneveld, A.-J., Veerman, H., & Pannekoek, H. (1986a) *J. Biol. Chem. 261*, 14214–14218.
Wagner, G. (1990) *Prog. Nucl. Magn. Reson. Spectrosc. 22*, 101–139.
Winn, E. S., Hu, S.-P., Hochschwender, S. M., & Laursen, R. A. (1980) *Eur. J. Biochem. 104*, 579–586.
Wu, T. P., Padmanabhan, K., Tulinsky, A., & Mulichak, A. M. (1991) *Biochemistry 30*, 10589–10594.
Wüthrich, K. (1986) *NMR of Proteins and Nucleic Acids*, John Wiley & Sons, Inc., New York.

Registry No. Urokinase, 9039-53-6.